Last glacial cycle glacier erosion potential in the Alps

Julien Seguinot[1] and Ian Delaney[2]

[1]Independent scholar, Anafi, Greece
[2]Institute of Earth Surface Dynamics, University of Lausanne, Switzerland

Abstract.

The glacial landscape of the Alps has fascinated generations of explorers, artists, mountaineers and scientists with its diversity, including erosional features of all scales from high-mountain cirques, to steep glacial valleys and large over-deepened basins. Using previous glacier modelling results, and empirical inferences of bedrock erosion under modern glaciers, we compute a distribution of potential glacier erosion in the Alps over the last glacial cycle from 120 000 years ago to the present. Despite large uncertainties pertaining to the climate history of the Alps and unconstrained glacier erosion processes, the resulting modelled patterns of glacier erosion include persistent features. The cumulative imprint of the last glacial cycle shows a very strong localization of glacier erosion with local maxima at the mouths of major Alpine valleys and some other upstream sections where glaciers are modelled to have flown with the highest velocity. The modelled erosion rates vary significantly through the glacial cycle, but show paradoxically little relation to the total glacier volume. Phases of glacier advance and maximum extension see a localization of rapid erosion rates at low elevation, while glacier erosion at higher elevation is modelled date from phases of less extensive glaciation. The modelled erosion rates peak during deglaciation phases, when frontal retreat results in steeper glacier surface slopes, implying that climatic conditions that result in rapid glacier erosion might be quite transient and specific. Our results depict the Alpine glacier erosion landscape as a time-transgressive patchwork, with different parts of the range corresponding to different glaciation stages and time periods.

1 Introduction

The glacial erosion landscape of the Alps has fascinated generations of explorers, artists, mountaineers and scientists for centuries. Its cultural impact is indeed so far-reaching, that in English, a non-Alpine language, the adjective "alpine" with non-capital "a" is now casually used to describe an Alpine-like, glacially modified mountain landscape outside the Alps, while the proper noun "Alps" has been applied to nick-name Alpine-like, glacier eroded mountain ranges in Norway (*Lyngsalpene*), New Zealand (Southern Alps), Japan (日本アルプス, *Nihon Arupusu*), and elsewhere. Some mountain ranges are predominantly characterised by cirque glaciation (e.g. Uinta Mountains), glacial valleys (e.g. Putorana Plateau), or large-scale overdeepenings (e.g. Patagonia). But other regions, including the Alps, present a higher variety of glacier erosional landforms (Ramsay, 1862; Ball, 1863; Gastaldi, 1873; Penck, 1905, Fig. 1) whose implications on glacial history is yet to be understood. The cosmogenic nuclide memory of bedrock erosion provides a more quantitative, yet equally varied picture of glacier erosion effectiveness both within and between glaciated regions (Jansen et al., 2019; Steinemann et al., 2020, 2021).

Figure 1. Alpine glacial erosion landscape diversity. **(a)** Piedmont overdeepening of Lake Constance, ca. 10x50 km. **(b)** Glacial trough of Lauterbrunnental, ca. 1x10 km. **(c)** Mountain cirque of Chüebodengletscher, ca. 1x1 km.

In absence of other landforms, glacially eroded topography has sometimes been used as a proxy for glacier extent, for instance in geomorphological mapping (e.g., Margold et al., 2011; Fu et al., 2012). Cold-based glaciers, however, have been observed to preserve landforms as fragile as sand beaches (Kleman, 1994), leading to the reinterpretation of complex glacial landscapes within a binary conceptual framework of cold and temperate basal thermal regimes (Kleman et al., 2008, 2010; Fabel et al., 2012; Fu et al., 2013). Nevertheless, it remains unclear how sharp the erosional transition to cold-based ice is, and why some glaciated regions show characteristic landform preservation and others, including the Alps, do not (Wirsig et al., 2016; Seguinot et al., 2018).

Glacier erosion also likely governs, at least in part, the height of mountains (Egholm et al., 2009; Thomson et al., 2010) through the "glacier buzz-saw". In turn, evidence suggests that increased mountain erosion rates coincided with global cooling and Pleistocene glaciations from roughly 2.6 million years before present (Herman and Champagnac, 2016). Yet, oceanic isotopic proxies for global weathering rates remained constant over this time period (Willenbring and Von Blanckenburg, 2010). Examination of contemporary erosion rates across different climates suggest that increased temperatures in glaciated regions lead to higher erosion rates and that erosion rates may have increased towards present (Koppes and Montgomery, 2009; Koppes et al., 2015; Fernandez et al., 2016). However, understanding the link between climate and glacier erosion in the sedimentary record remains difficult due to time scale biases (Ganti et al., 2016) and the non-linear relationship between atmospheric temperature and erosion (e.g., Anderson et al., 2012; Mariotti et al., 2021).

Observing and quantifying the long-term glacier erosion and sedimentation processes has been a challenge, and two general methods have been adopted to quantify erosion (Alley et al., 2019). Physically-based models describe quarrying process and abrasion of bedrock by debris laden ice (e.g., Alley et al., 1997; Iverson, 2012; Beaud et al., 2014). Describing the processes physically provides a basis for understanding erosion processes (Hallet, 1979; Ugelvig et al., 2018) and yields insight into the formation of glacial landforms, such as tunnel valleys and eskers (Beaud et al., 2018; Hewitt and Creyts, 2019). Yet, these models prove difficult to implement in many cases due to the large number of poorly constrained parameters and process, i.e. water pressure fluctuations and subglacial debris concentration (e.g., Hallet, 1979; Seguinot, 2008; Ugelvig et al., 2018).

50   Instead, empirical relationships between glacier sliding and erosion can represent erosional quantities well and can recreate important glacial landforms (e.g., Harbor et al., 1988; MacGregor et al., 2000). For instance, Humphrey and Raymond (1994) correlated temporal variations in ice velocity and suspended sediment load during a surge of Variegated Glacier to establish a linear erosion law. Koppes et al. (2015) quantified sediment yields in 15 Patagonian and Antarctic Peninsula fjords, concluding at a predominant control of surface air temperature on rapid glacier erosion and calibrating a near-square-law from glacier

55   velocity to erosion rate. Herman et al. (2015) collected suspended sediment samples for 5 months in the outlet stream of Franz-Josef Glacier, mapped their chemical composition to geologic zones of distinctive glacier speed, and also concluded to a near-square relationship between basal sliding and glacier erosion. Cook et al. (2020) assembled a global compilation of erosion rates for 38 glaciers, showing a predominant role of glacier sliding velocity over climate variables, yet concluding at a sub-linear relationship to erosion.

60   Here, the non-linear erosion law by Koppes et al. (2015) is applied to previously published model results (Seguinot et al., 2018) and the patterns of modelled erosion rates and cumulative last glacial cycle erosion potential are analysed. We examine the glaciological conditions that cause erosion and discuss the implications of these conditions on understanding the relationship between climate and glacier erosion. Despite aggregated uncertainties on paleoclimate, glacier flow and glacier erosion processes, out results provide insights into the diversity of the Alpine glacial erosion landscape.

2   Methods

2.1   Ice sheet modelling

The ice-sheet model set-up was presented in an earlier publication (Seguinot et al., 2018) and is briefly summarized here. The simulations were conducted using the Parallel Ice Sheet Model (PISM, development version e9d2d1f), an open-source, finite-difference, shallow-ice and shallow-shelf model (the PISM authors, 2017). Our setup includes temperature and water-

70   content dependent creep, pseudo-plastic basal sliding, bedrock deformation under the ice load, and a positive degree-day (PDD) surface mass balance model. The model is initialized with assumed present-day ice thickness and equilibrium ice and bedrock temperature at 120 ka (thousand years before the present), and ran to the present. The ice-sheet model physical parameters are listed in the earlier open-access publication (Seguinot et al., 2018), and the complete list of PISM parameters is stored in long-term archived model output metadata for the present study (Seguinot, 2021), and for the earlier publication (Seguinot,

75   2020a, b).

Climate forcing is provided by a monthly climatology from interpolated observational data (WorldClim; Hijmans et al., 2005) and the European Centre for Medium-Range Weather Forecasts Reanalysis Interim (ERA-Interim; Dee et al., 2011), amended with temperature lapse-rate corrections from the European Project for Ice Coring in Antarctica (EPICA; Jouzel et al., 2007), and time-dependent paleo-precipitation reductions (Huybrechts, 2002). Lower-resolution runs based on alternative

80   paleoclimate scenarios (Seguinot et al., 2018) are analyzed in the discussion part (Sect. 4.1).

2.2 Erosion law

Modelled erosion rates, $\dot{e}$, are calculated from the modelled basal velocities, u_b, using a empirical erosion power-law,

$$\dot{e} = K_g u_b^l, \tag{1}$$

where $K_g = 5.2 \times 10^{-11}\,m^{1-l}\,a^{l-1}$ and $l = 2.34$ are empirical constants calibrated on quantified fjord sediment yields and
85 velocities from 15 Patagonian and Antarctic Peninsula tidewater glaciers (Koppes et al., 2015). We discuss the role of alternative
values of K_g and l in the discussion part (Sect. 4.2).

Our approach does not account for feedbacks of glacier erosion onto bedrock topography and, then onto, ice dynamics (e.g.,
Anderson et al., 2012). Furthermore, we assume that once material is eroded, it is transported out of the system. In turn, we
do not account for the downstream advection of debris (e.g., Anderson and Anderson, 2016), or fluvial transport of subglacial
90 sediment (Delaney et al., 2019). Instead, we compute the time-integrated glacier erosion rate,

$$e = K_g \int u_b^l dt, \tag{2}$$

and refer to it as the cumulative "erosion potential". The integration is numerically approximated using a time-step of 10 a in
the main simulation, and 100 a in the alternative climate scenarios runs. Note that in the above formula with an exponent, l,
higher than one, the cumulative erosion potential has a greater dependency on the basal ice dynamics, u_b, than the duration of
95 glacier cover.

3 Results

3.1 Cumulative erosion

The modelled cumulative (time-integrated) glacial erosion potential (Fig. 2a) varies by several orders of magnitude from in-
significant to hundred-metres-scale erosion potential. Its spatial patterns show a very strong localization along the Alpine
100 valleys, with local maxima occurring both at the Alpine gates where ice flow transited from valley to piedmont glaciers, and
further upstream where the valley slopes increase. While mountain cirques are poorly captured by the model's horizontal res-
olution, high cumulative erosion potential also occurs near the valley heads. There is a general tendency for higher cumulative
erosion in the north-western Alps where the input winter precipitation is higher (WorldClim, Fig. 1h in Seguinot et al., 2018)
and the glacial relief more pronounced in the topography.

3.2 Temporal evolution

105

The modelled annual (domain-integrated) glacial erosion volume does not systematically correlate with the modelled total
ice volume (Fig. 2b). Except for the onset and termination of the glacial cycle were ice volume is low and sliding processes
unlikely to be captured by the model resolution, a comparison between the modelled ice volume and the modelled annual
erosion volume shows no single relation between these two quantities (Fig. 3). After significant ice volume has been reached,
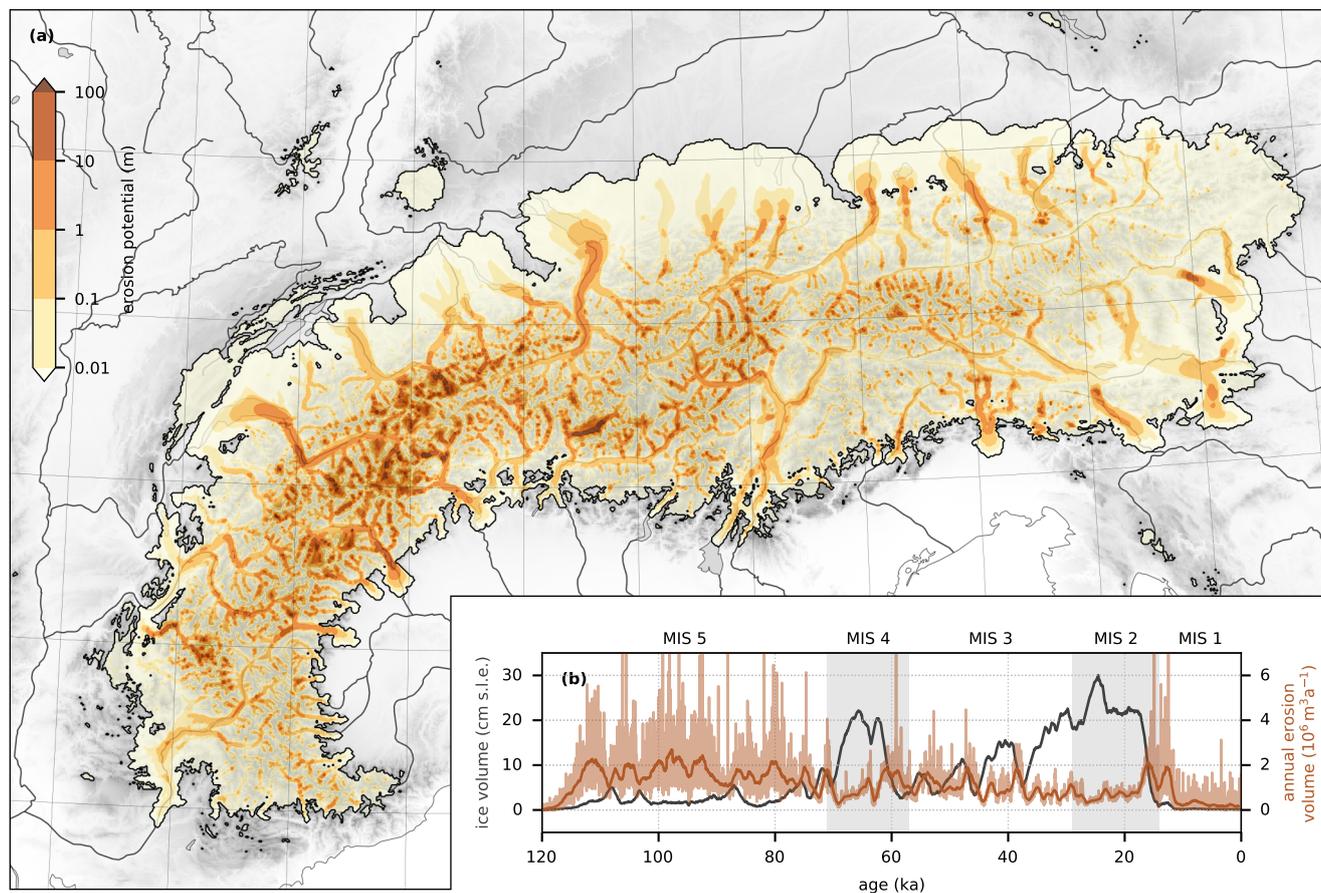
Figure 2. (a) Modelled cumulative (time-integrated) glacial erosion potential over the last glacial cycle. **(b)** Modelled total ice volume in centimetres of sea-level equivalent (cm s.l.e., black), annual (domain-integrated) erosion volume (light brown) and 1-ka running mean (dark brown). Shaded gray areas indicate the timing for MIS 2 and 4 (Lisiecki and Raymo, 2005).

there is a slight tendency for slower erosion during periods of extensive glaciation (Fig. 3). However, the domain-integrated erosion volume is modelled to be consistently higher (by a factor 2 to 10) during periods of decreasing ice volume, than during periods of increasing ice volume (Fig. 3).

3.3 Spatial migration

A closer look at the Rhine Glacier, one of the paleo-ice sheet's largest outlets, reveals a spatial migration of the modelled rapid erosion areas. During stages of glacier advance and maximum extension, erosion is modelled to be under $1\,\mathrm{mm\,a^{-1}}$ and restricted the lower parts of the catchment, while much the intra-montane Alps (modelled to be largely cold-based, Fig. 6c in Seguinot et al., 2018), experience insignificant erosion (Fig. 4a and d). The modelled erosion rates both increase and propagate inwards during periods of glacier retreat (Fig. 4b, c and d).
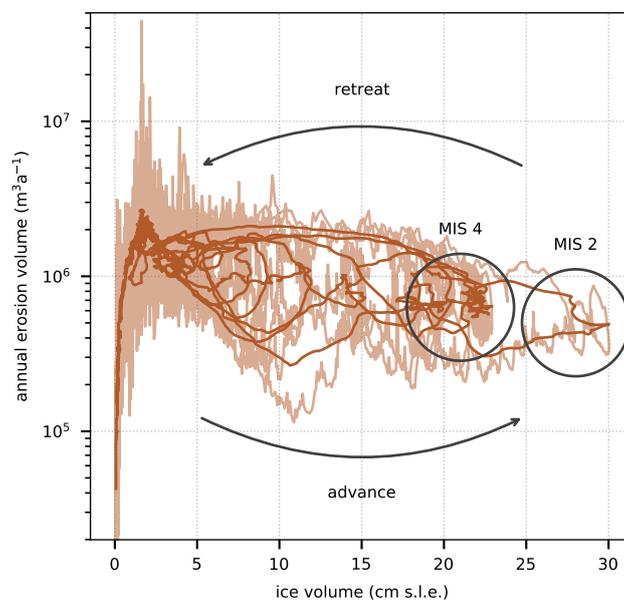
Figure 3. Modelled annual (domain-integrated) erosion volume (light brown) and 1-ka running mean (dark brown) in relation to modelled total ice volume in centimetres of sea-level equivalent.
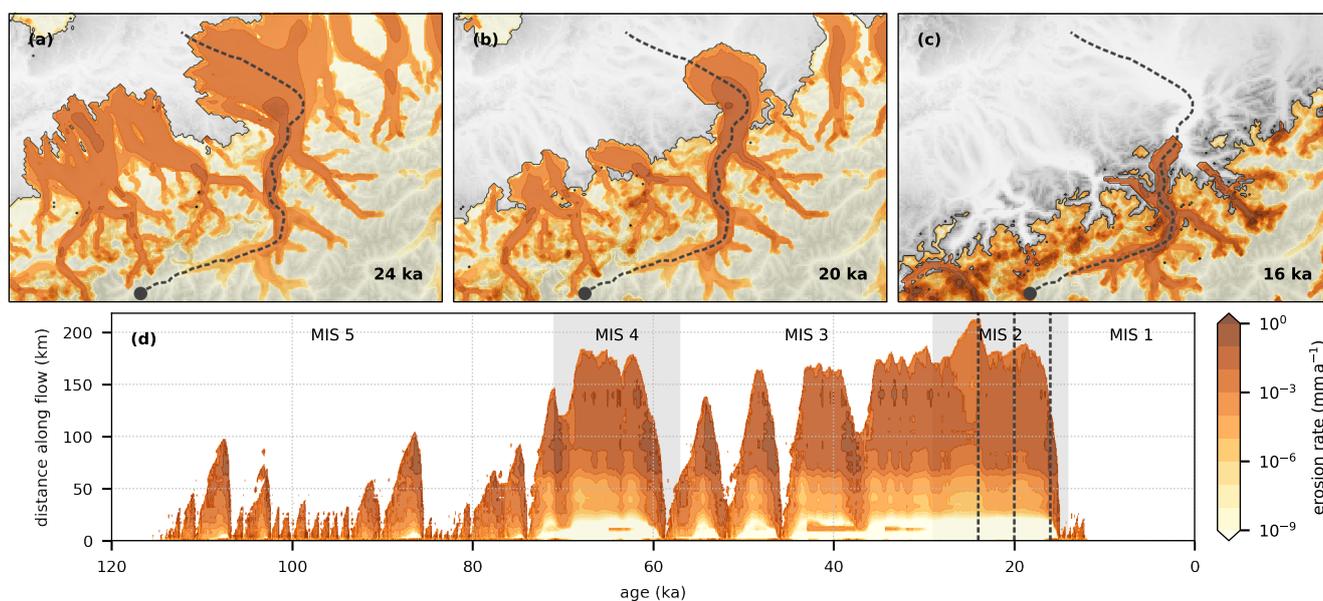
Figure 4. (a, b, c) Modelled instantaneous erosion rate of the Rhine Glacier for selected post-Last Glacial Maximum ages. **(d)** Interpolated instantaneous erosion rate along a Rhine Glacier transect for the entire last glacial cycle (upper panels dashed line).
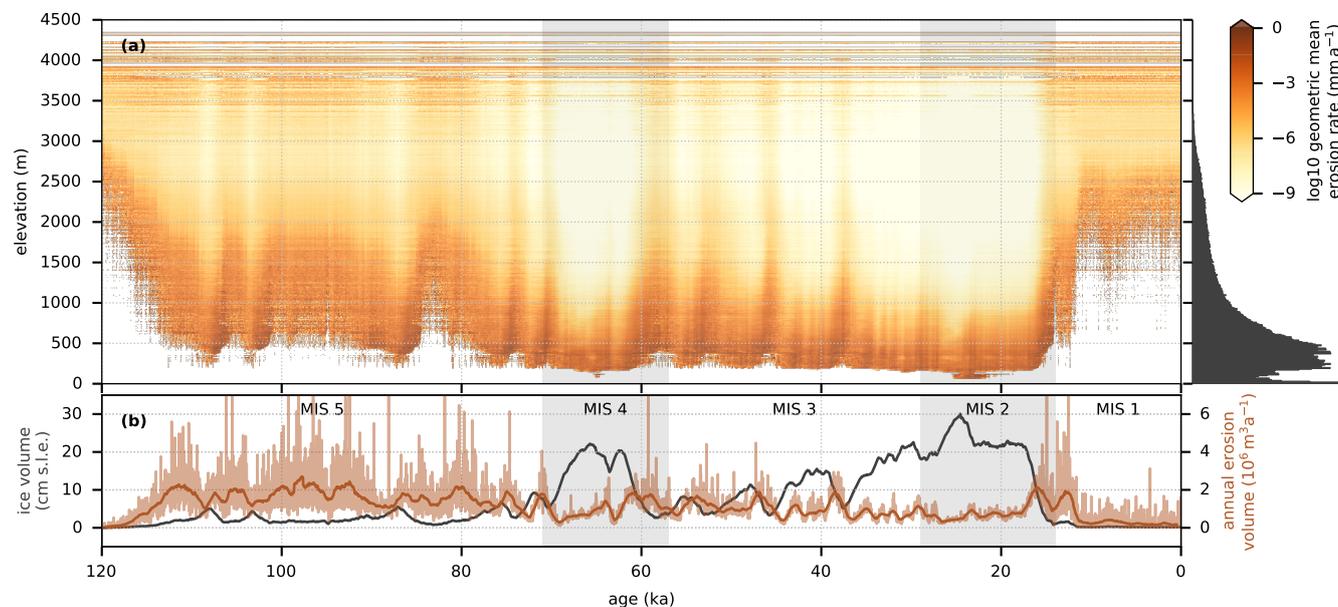
Figure 5. (a) Modelled erosion rate "hypsogram", showing the geometric mean of (non-zero) modelled erosion rates in 10-m elevation bands across the entire model domain and its time evolution. The histogram to the side shows the distribution of topography in the model domain. **(b)** Same as Fig. 2b.

The results found on the Rhine Glacier catchment can be generalized to the entire model domain by using (present-day) bedrock altitude as a proxy for along-flow distance (Fig. 5). Thus more generally, periods of modelled increasing and maximum ice volume correspond to lower values for elevation-aggregated erosion rates, with significant erosion restricted to lower elevations. On the opposite, periods of modelled decreased ice volume correspond to higher local modelled erosion rates and more extensive rapid erosion into higher-elevation areas (Fig. 5).

4 Discussion

4.1 Climate sensitivity

Different paleoclimate forcing scenarios lead to different modelled glaciation histories (cf. Seguinot et al., 2018) and thus different results in terms of erosion potential (Fig. 6). Scenarios including higher (constant, present-day) input precipitation rates yield generally higher modelled erosion potential (Fig. 6a, b, and c), while scenarios including paleo-precipitation reductions (Fig. 6d, e, and f), including our default high-resolution run (Fig. 2), yield a smaller erosion potential. The spatial pattern of modelled time-integrated erosion is nevertheless generally consistent across the paleoclimate scenarios tested, despite variations in the glaciation maximum extent (Fig. 3 in Seguinot et al., 2018; Fig. 6). Furthermore, these changes are minor considering the large uncertainties affecting the choice of erosion law.
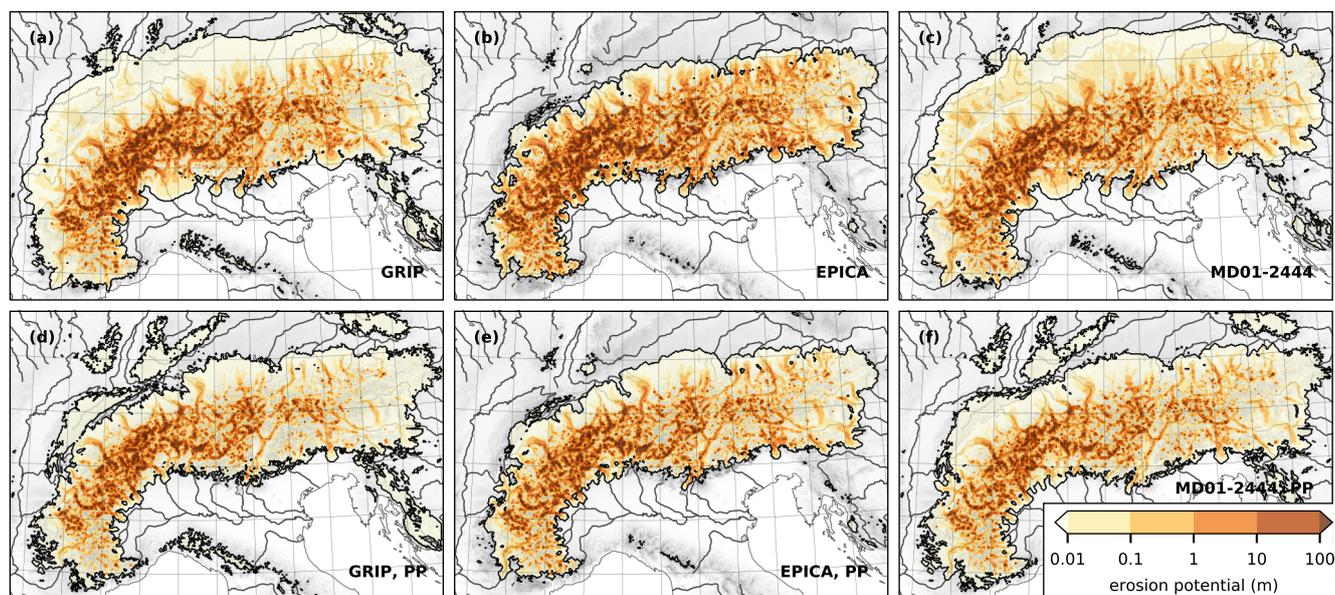
Figure 6. Modelled cumulative glacial erosion potential over the last glacial cycle without **(a, b, c)** and with **(d, e, f)** paleo-precipitation corrections, and using three different palaeo-temperature histories (see Seguinot et al., 2018).

4.2 Choice of erosion law

The choice of erosion law significantly impacts the results (Fig. 7). Our default, based on quantified sediment yields from Patag-
onian and Antarctic Peninsula tidewater glaciers ($\dot{e} = 5.2 \times 10^{-8} u_{\mathrm{b}}^{2.34}$, Koppes et al., 2015) yields a moderate and strongly
localized cumulative erosion potential (Figs 2 and 7a). The erosion law based on measured suspended sediment load from
Franz-Joseph Glacier ($\dot{e} = 2.7 \times 10^{-7} u_{\mathrm{b}}^{2.02}$, Herman et al., 2015) also yields a strongly localized, and yet much higher, mod-
elled erosion potential (Fig. 7b). The erosion law based on measured suspended sediment load during a surge of Variegated
Glacier ($\dot{e} = 1 \times 10^{-4} u_{\mathrm{b}}^{1}$, Humphrey and Raymond, 1994) results in similarly high values, but a less localized pattern of cu-
mulative erosion potential (Fig. 7c). Finally, The erosion law based on a global compilation of glacier velocities and erosion
rates ($\dot{e} = 1.665 \times 10^{-1} u_{\mathrm{b}}^{0.6459}$, Cook et al., 2020) yields an even flatter pattern of cumulative erosion potential (Fig. 7d).

It may seem surprising that the erosion law calibrated on Patagonian and Antarctic Peninsula tidewater glaciers (Koppes
et al., 2015) yields a more realistic glacial cycle erosion potential in the Alps than those based on terrestrial glaciers (Humphrey
and Raymond, 1994; Herman et al., 2015; Cook et al., 2020), themselves resulting in kilometre-scale integrated erosion even
higher than the Alpine relief itself. However, during the Last Glacial Maximum and much of the last glacial cycle, Alpine
paleoglaciers were closer in size, slope, and climatic context to the present-day glaciers of Patagonia and the Antarctic Penin-
sula (Koppes et al., 2015) than to Franz-Joseph Glacier (Herman et al., 2015) and many of the glaciers included in the global
compilation by Cook et al. (2020).

Earth **Surface**
Dynamics
Discussions
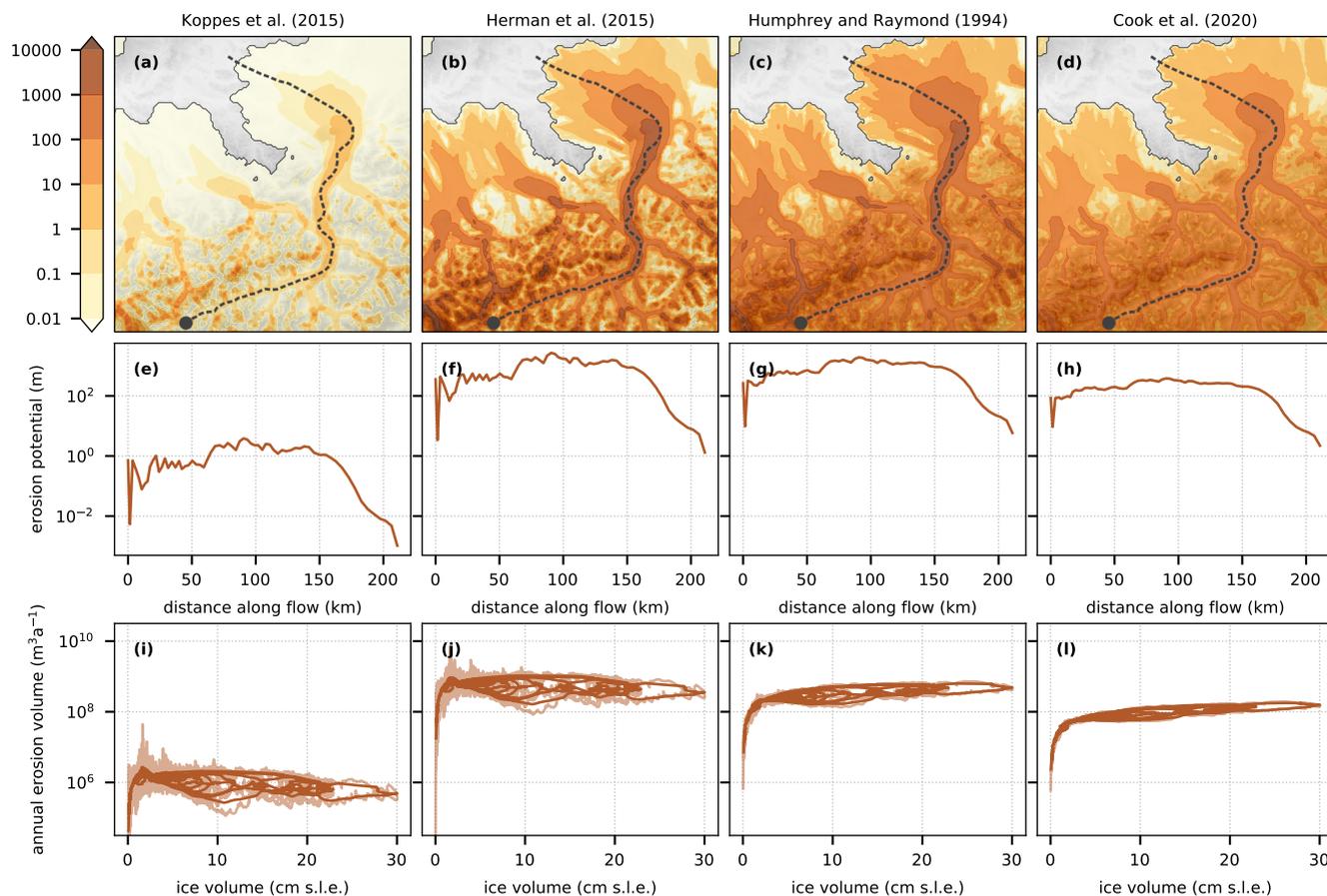
Figure 7. Modelled cumulative (time-integrated) glacial erosion potential for three different erosion laws published by **(a)** Koppes et al. (2015), $5.2 \times 10^{-8} u_{\mathrm{b}}^{2.34}$ (same as Fig. 2a but with a different colour scale), **(b)** Herman et al. (2015), $2.7 \times 10^{-7} u_{\mathrm{b}}^{2.02}$, **(c)** Humphrey and Raymond (1994), $1 \times 10^{-4} u_{\mathrm{b}}^{1}$, and **(d)** Cook et al. (2020), $1.665 \times 10^{-1} u_{\mathrm{b}}^{0.6459}$. **(e-h)** Corresponding modelled cumulative glacial erosion potential along a Rhine Glacier transect (upper panels dashed line), and **(i-l)** corresponding modelled evolution of annual (domain-integrated) erosion volume (light brown) and 1-ka running mean (dark brown) in relation to modelled total ice volume in centimetres of sea-level equivalent (as in Fig. 3a).

That said, the magnitude of the modelled erosion rates can hardly be used as a criteria to rule out this or that erosion law
150   for the glacial Alps. While sliding is here modelled by a pseudo-plastic law based on till dilatation under high water pressure
(Tulaczyk et al., 2000), empirical erosion rules are thought to be a proxy for glacier abrasion (cf. Hallet, 1979; and possibly
plucking) of a glacier flowing over a hard bed. Current erosion rates in the Alps strongly vary depending on the substratum
(Steinemann et al., 2020, 2021), and it arguable that a layer of till and proglacial sediments may have armored the glacier bed
from erosion for at least parts of the glacial cycle. Given the lack of data to constrain the erosion rule, it can not be excluded that
155   a linear or sub-linear erosion-law (e.g., Cook et al., 2020) would lead to a less localized pattern of erosion (Fig. 7c and d), and
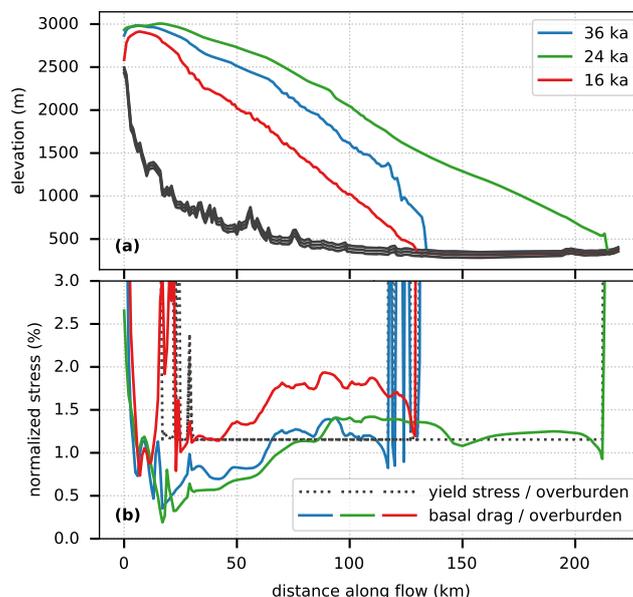
Figure 8. (a) Modelled basal and surface topographies interpolated along the Rhine Glacier during glacier advance (36 ka), maximum extent (24 ka) and retreat (16 ka, using the same transect as in Fig. 8). **(b)** Interpolated yield stress in the pseudo-plastic sliding law (dotted lines) and magnitude of the basal shear stress (basal drag, solid lines), both normalized against the ice overburden pressure. Basal drag values greater than yield stress result in glacier sliding (cf. Seguinot, 2014; Seguinot et al., 2016, for model physics).

a stronger correlation between modelled ice volume and erosion (Fig. 7k and l). Even then, the intrinsically large variations in modelled glacier sliding velocities yield cumulative glacial-cycle erosion two to three orders of magnitude higher in the Alpine valleys than near the mountain tops (Fig. 7d). Yet this result is compatible with the order-of-magnitude variation of glacier erosion rates observed in the cosmogenic nuclide record (Jansen et al., 2019; Steinemann et al., 2020, 2021).

4.3 Climate control on erosion

160

The modelled, domain-integrated glacier erosion volume do not increase together with ice volume. On the opposite, periods of ice advance and maximum glaciation correspond to comparatively slow erosion (Figs. 2 and 3). This result may seem paradoxical, and is modulated in a limited extent by the exponent, l, in the erosion rule (Fig. 7). During deglaciation periods, increased surface melt at low elevations results in a steepened topographic profile (Figs. 8a), as observed and further expected

165 on currently retreating glaciers (Huss et al., 2010; Zekollari and Huybrechts, 2015). The buttress formed by the glacier foot against gravitational forces is reduced, causing an increase in the magnitude of the basal shear stress (basal drag) relative to the ice overburden pressure, and an increase in the area where sliding and thus, erosion, can occur (Figs. 8b).

This result is corroborated by a recent denudation record from the Mediterranean Alps, which includes an increase in glacier erosion in the Var Valley, roughly at 25 ka following an extended period of low denudation rates (Mariotti et al., 2021). While

170   that increase in erosion predates the increase observed in our study (ca. 15 ka; Fig. 3), it demonstrates that climatic conditions over-which glacier erosion occurs are relatively specific and likely transient. Other field-based studies have evidenced increased glacier erosion and pro-glacial sedimentation during the current deglaciation period (e.g., Koppes and Montgomery, 2009; Micheletti and Lane, 2016; Lane et al., 2017; Bendixen et al., 2017). Yet this increase has often been attributed to higher meltwater availability, promoting sediment transport (Delaney and Adhikari, 2020), enhanced glacier sliding (Herman et al.,
175   2011), and hydrofracturing, i.e. plucking (Hallet, 1996; Ugelvig et al., 2018; Hildes et al., 2004).

But importantly, these hydrological processes are not included in our model, so that deglaciation surface meltwater is assumed to instantly exit the glacier with no effect on glacier dynamics (cf. Werder et al., 2013; Iverson, 2012; Ugelvig et al., 2018, for comparison). The enhanced glacier velocity during periods of ice retreat is here modelled to result from changes in glacier geometry alone (Figs. 8b). Observed feedbacks between surface meltwater and basal sliding, not included in the model,
180   presumably further accelerated erosion during deglaciation (Herman et al., 2011). Furthermore, we omit the fluvial transport of sediment, which could well increase sediment discharge and erosion with increased melt, so long as additional sediment remains available (Delaney and Adhikari, 2020). Rapid glacier erosion can be expected to accompany the ongoing 21st-century deglaciation, especially for the ice sheets of Greenland and Antarctica where polythermal and cold-based glaciers are warming and sliding may increase (e.g., Moon et al., 2012; Mouginot et al., 2014; Overeem et al., 2017).

185   ## 4.4 Age of the glacial landscape

In many places throughout the Alps, significant modelled cumulative erosion occurs far inside the Alpine valleys (Fig. 2). Yet instantaneous erosion rates show a time-transgressive radial pattern (Fig. 4), so that high-altitude rapid erosion is not modelled to date from expansive glaciation stages, but instead to stages of intermediate glacier cover (Fig. 5; Barr et al., 2019).

For instance, low-elevation piedmont over-deepened basins such as Lake Constance (Fig. 1), Lake Geneva and Lake Mag-
190   giore, are here modelled to be the product of extensive, Last Glacial Maximum-like glaciations. Other modeling work suggests that features such as these likely form when water can access the glacier bed and encourage glacier sliding and, thus, erosion (Herman et al., 2011). The model herein does not include subglacial hydrology, yet the role of climate warming to increasing glacier erosion to the lower elevations remains evident (Fig. 5). Alpine terrain with elevations above 1000 m are modelled to experience virtually no erosion from 35 to 18 ka BP (Fig. 5), so that many of the most spectacular, intermediate-elevation
195   glacial valleys of the Alps as Lauterbrunnental (Fig. 1), Haslital (Upper Aare) or Bout du Monde (Upper Giffre) would date from periods of intermediate glacier extension. While the validity of the model results at high elevation are limited by the 1-km resolution and the shallow-ice physics (Imhof et al., 2019), the lack of rapid erosion at high-elevations for much of the modelled glacial cycle implies that the numerous Alpine mountain cirques such as Chüebodensee (Fig. 1) would have formed over interglacial periods, when glaciers are confined to their cirques (Barr et al., 2017, 2019). Similar processes also occur on
200   Himalayan glaciers and may limit erosion for the high elevation portion of that mountain range during cold periods as well, failing to offset uplift rates (Harper and Humphrey, 2003).

Finally, the time-transgressive nature of the modelled glacial erosion rates hint at a new explanation for the Alpine glacier trim-line and lack of cold-based glaciation evidence. Due to their geographic location in the mid-latitudes, and their steep

topographic gradient, the Alps appear as a mountain range that hosted glaciers of various sizes throughout the varying climate of the Quaternary, resulting in a transgressive localization of glacier erosion throughout their elevational range, from the piedmont during glacial maxima, to the highest cirques during interglacial periods. The Alpine trim-line, in this case, would neither correspond to the upper reach of the Last Glacial Maximum glaciers (e.g., Kelly et al., 2004), nor to an englacial temperate-ice boundary (Coutterand, 2010; Seguinot et al., 2018), but to a time-transgressive upper limit of erosion from retreating glaciers on steep terrain.

5 Conclusions

Due to compounded uncertainties regarding paleoclimate, glacier sliding and erosion processes, our quantitative results are very likely inaccurate. Yet, we draw the following qualitative conclusions:

- The non-linear physics of glacier deformation and sliding, combined with non-linear empirical erosion laws, results in a very strong localization of rapid glacier erosion in regions of fast flow.

- This high spatio-temporal variability hints at a complex relationship between climate and glacier erosion, so that a highly variable response of glacier erosion to climate should be expected.

- Increased gravitational drag due to surface profile steepening provide a mechanism for accelerated erosion during deglaciation periods, irrespective of surface meltwater penetration to the glacier bed.

- If a non-linear glacier erosion law is used, the climate-induced slowdown of erosion counterbalances glacier expansion, so that Alpine-wide glacier erosion volumes do not correlate with the ice volume.

- Rapid glacier erosion is restricted to low elevation during stages of glacier advance and maximum glaciation, but propagates up-valley to higher elevations during periods of glacier retreat.

- The diversity of the Alpine glacier erosion landscape appears to be the time-transgressive signature of a variety of glacial stages ranging from pan-Alpine ice sheets to modern-style mountain glaciers.

Code and data availability. PISM is available as open-source software (http://pism-docs.org). Time and domain-aggregated erosion variables such as used in the figures is available for the four presented erosion power-laws (https://doi.org/10.5281/zenodo.4495419). Other model output variables were previously made available (https://doi.org/10.5281/zenodo.3604174, https://doi.org/10.5281/zenodo.3604142).

Video supplement. Animations made available online show the modelled glacier erosion rates (https://vimeo.com/503162771), and their evolving relationship with ice volume (https://vimeo.com/512478926) and bedrock altitude (https://vimeo.com/512479008).

230 *Author contributions.* J. Seguinot performed the computations and prepared the figures. I. Delaney interpreted the results in a broader context. Both authors contributed to the text.

Competing interests. The authors declare that they have no conflict of interest.

Acknowledgements. We are very thankful to Constantine Khroulev, Ed Bueler, and Andy Aschwanden for their constant help and development with PISM, without whom this work would not have been possible. J. Seguinot would like to thank John Jansen and Martin Margold
235 for insightful early discussions, Susan Ivy-Ochs for being a constant (droid) motivator, Popi, Karsta and Stefan for welcoming him on Anafi and providing agreeable conditions for work in times of pandemic, and the Long Haul Trucker for conveying his laptop and data unbroken for 5000 km across Europe and fourteen countries. I. Delaney thanks Frédéric Herman for valuable support and conversations while at University of Lausanne. The (previously published) ice flow simulations were made with computer resources provided by the Swiss National Supercomputing Centre (CSCS) allocations no. s573 and sm13 to J. Seguinot.

References

Alley, R. B., Cuffey, K. M., Evenson, E. B., Strasser, J. C., Lawson, D. E., and Larson, G. J.: How glaciers entrain and transport basal sediment: physical constraints, Quaternary Sci. Rev., 16, 1017–1038, https://doi.org/10.1016/S0277-3791(97)00034-6, 1997.

Alley, R. B., Cuffey, K. M., and Zoet, L. K.: Glacial erosion: status and outlook, Ann. Glaciol., 60, 1–13, https://doi.org/10.1017/aog.2019.38, 2019.

Anderson, L. and Anderson, R.: Modeling debris-covered glaciers: response to steady debris deposition, The Cryosphere, 10, 1105, https://doi.org/10.5194/tc-10-1105-2016, 2016.

Anderson, R., Dühnforth, M., Colgan, W., and Anderson, L.: Far-flung moraines: Exploring the feedback of glacial erosion on the evolution of glacier length, Geomorphology, 179, 269–285, https://doi.org/10.1016/j.geomorph.2012.08.018, 2012.

Ball, J.: XII. On the formation of alpine valleys and alpine lakes, London Edinburgh Dublin Phil. Mag. J. Sci., 25, 81–103, https://doi.org/10.1080/14786446308643424, 1863.

Barr, I., Ely, J., Spagnolo, M., Clark, C., Evans, I., Pellicer, X., Pellitero, R., and Rea, B.: Climate patterns during former periods of mountain glaciation in Britain and Ireland: Inferences from the cirque record, Palaeogeogr., Palaeoclimatol., Palaeoecol., 485, 466 – 475, https://doi.org/10.1016/j.palaeo.2017.07.001, 2017.

Barr, I., Ely, J., Spagnolo, M., Evans, I., and Tomkins, M.: The dynamics of mountain erosion: cirque growth slows as landscapes age, Earth Surf. Processes and Landforms, 44, 2628–2637, https://doi.org/10.1002/esp.4688, 2019.

Beaud, F., Flowers, G. E., and Pimentel, S.: Seasonal-scale abrasion and quarrying patterns from a two-dimensional ice-flow model coupled to distributed and channelized subglacial drainage, Geomorphology, 219, 176–191, https://doi.org/10.1016/j.geomorph.2014.04.036, 2014.

Beaud, F., Venditti, J., Flowers, G., and Koppes, M.: Excavation of subglacial bedrock channels by seasonal meltwater flow, Earth Surf. Processes and Landforms, 43, 1960–1972, https://doi.org/10.1002/esp.4367, 2018.

Bendixen, M., Iversen, L. L., Bjørk, A. A., Elberling, B., Westergaard-Nielsen, A., Overeem, I., Barnhart, K. R., Khan, S. A., Abermann, J., Langley, K., et al.: Delta progradation in Greenland driven by increasing glacial mass loss, Nature, 550, 101, https://doi.org/10.1038/nature23873, 2017.

Cook, S. J., Swift, D. A., Kirkbride, M. P., Knight, P. G., and Waller, R. I.: The empirical basis for modelling glacial erosion rates, Nature Communications, 11, https://doi.org/10.1038/s41467-020-14583-8, 2020.

Coutterand, S.: Etude géomorphologique des flux glaciaires dans les Alpes nord-occidentales au Pléistocène récent : du maximum de la dernière glaciation aux premières étapes de la déglaciation, Ph.D. thesis, Université de Savoie, 2010.

Dee, D. P., Uppala, S. M., Simmons, A. J., Berrisford, P., Poli, P., Kobayashi, S., Andrae, U., Balmaseda, M. A., Balsamo, G., Bauer, P., Bechtold, P., Beljaars, A. C. M., van de Berg, L., Bidlot, J., Bormann, N., Delsol, C., Dragani, R., Fuentes, M., Geer, A. J., Haimberger, L., Healy, S. B., Hersbach, H., Hólm, E. V., Isaksen, L., Kållberg, P., Köhler, M., Matricardi, M., McNally, A. P., Monge-Sanz, B. M., Morcrette, J.-J., Park, B.-K., Peubey, C., de Rosnay, P., Tavolato, C., Thépaut, J.-N., and Vitart, F.: The ERA-Interim reanalysis: configuration and performance of the data assimilation system, Q. J. Roy. Meteor. Soc., 137, 553–597, https://doi.org/10.1002/qj.828, 2011.

Delaney, I. and Adhikari, S.: Increased subglacial sediment discharge during century scale glacier retreat: consideration of ice dynamics, glacial erosion and fluvial sediment transport, Geophys. Res. Lett., p. e2019GL085672, https://doi.org/10.1029/2019GL085672, 2020.

Delaney, I., Werder, M. A., and Farinotti, D.: A numerical model for fluvial transport of subglacial sediment, J. Geophys. Res. Earth Surf., 124, 2197–2223, https://doi.org/10.1029/2019jf005004, 2019.

Egholm, D., Nielsen, S., Pedersen, V., and Lesemann, J.-E.: Glacial effects limiting mountain height, Nature, 460, 884–887, https://doi.org/10.1038/nature08263, 2009.

Fabel, D., Ballantyne, C. K., and Xu, S.: Trimlines, blockfields, mountain-top erratics and the vertical dimensions of the last British-Irish Ice Sheet in NW Scotland, Quaternary Sci. Rev., 55, 91–102, https://doi.org/10.1016/j.quascirev.2012.09.002, 2012.

280 Fernandez, R., Anderson, J., Wellner, J., Minzoni, R., Hallet, B., and Smith, R. T.: Latitudinal variation in glacial erosion rates from Patagonia and the Antarctic Peninsula (46 S–65 S), B. Geol. Soc. Am., 128, 1000–1023, https://doi.org/10.1130/B31321.1, 2016.

Fu, P., Heyman, J., Hättestrand, C., Stroeven, A. P., and Harbor, J. M.: Glacial geomorphology of the Shaluli Shan area, southeastern Tibetan Plateau, J. Maps, 8, 48–55, https://doi.org/10.1080/17445647.2012.668762, 2012.

Fu, P., Harbor, J. M., Stroeven, A. P., Hättestrand, C., Heyman, J., and Zhou, L.: Glacial geomorphology and paleoglaciation pat-
285 terns in Shaluli Shan, the southeastern Tibetan Plateau — Evidence for polythermal ice cap glaciation, Geomorphology, 182, 66–78, https://doi.org/10.1016/j.geomorph.2012.10.030, 2013.

Ganti, V., von Hagke, C., Scherler, D., Lamb, M., Fischer, W., and Avouac, J.-P.: Time scale bias in erosion rates of glaciated landscapes, Science Advances, 2, https://doi.org/10.1126/sciadv.1600204, 2016.

Gastaldi, S. B.: On the Effects of Glacier-erosion in Alpine Valleys, Q. J. Geol. Soc., 29, 396–401,
290 https://doi.org/10.1144/gsl.jgs.1873.029.01-02.30, 1873.

Hallet, B.: A theoretical model of glacial abrasion, J. Glaciol., 23, 39–50, https://doi.org/10.3189/s0022143000029725, 1979.

Hallet, B.: Glacial quarrying: a simple theoretical model, Ann. Glaciol., 22, 1–8, https://doi.org/10.3189/1996aog22-1-1-8, 1996.

Harbor, J. M., Hallet, B., and Raymond, C. F.: A numerical model of landform development by glacial erosion, Nature, 333, 347–349, https://doi.org/10.1038/333347a0, 1988.

295 Harper, J. and Humphrey, N.: High altitude Himalayan climate inferred from glacial ice flux, Geophys. Res. Lett., 30, https://doi.org/https://doi.org/10.1029/2003GL017329, 2003.

Herman, F. and Champagnac, J.-D.: Plio-Pleistocene increase of erosion rates in mountain belts in response to climate change, Terra Nova, 28, 2–10, https://doi.org/10.1111/ter.12186, 2016.

Herman, F., Beaud, F., Champagnac, J., Lemieux, J. M., and Sternai, P.: Glacial hydrology and erosion patterns: a mechanism for carving
300 glacial valleys, Earth Planet. Sc. Lett., 310, 498–508, https://doi.org/10.1016/j.epsl.2011.08.022, 2011.

Herman, F., Beyssac, O., Brughelli, M., Lane, S. N., Leprince, S., Adatte, T., Lin, J. Y. Y., Avouac, J.-P., and Cox, S. C.: Erosion by an Alpine glacier, Science, 350, 193–195, https://doi.org/10.1126/science.aab2386, 2015.

Hewitt, I. and Creyts, T.: A model for the formation of eskers, Geophys. Res. Lett., 46, 6673–6680, https://doi.org/10.1029/2019GL082304, 2019.

305 Hijmans, R. J., Cameron, S. E., Parra, J. L., Jones, P. G., and Jarvis, A.: Very high resolution interpolated climate surfaces for global land areas, Int. J. Climatol., 25, 1965–1978, https://doi.org/10.1002/joc.1276, 2005.

Hildes, D. H., Clarke, G. K., Flowers, G. E., and Marshall, S. J.: Subglacial erosion and englacial sediment transport modelled for North American ice sheets, Quaternary Sci. Rev., 23, 409–430, https://doi.org/10.1016/j.quascirev.2003.06.005, 2004.

Humphrey, N. F. and Raymond, C. F.: Hydrology, erosion and sediment production in a surging glacier: Variegated Glacier, Alaska, 1982–83,
310 J. Glaciol., 40, 539–552, https://doi.org/10.3189/s0022143000012429, 1994.

Huss, M., Jouvet, G., Farinotti, D., and Bauder, A.: Future high-mountain hydrology: a new parameterization of glacier retreat, Hydrology and Earth System Sciences, 14, 815–829, https://doi.org/10.5194/hess-14-815-2010, 2010.

Huybrechts, P.: Sea-level changes at the LGM from ice-dynamic reconstructions of the Greenland and Antarctic ice sheets during the glacial cycles, Quaternary Sci. Rev., 21, 203–231, https://doi.org/10.1016/s0277-3791(01)00082-8, 2002.

315 Imhof, M. A., Cohen, D., Seguinot, J., Aschwanden, A., Funk, M., and Jouvet, G.: Modelling a paleo valley glacier network using a hybrid model: an assessment with a Stokes ice flow model, J. Glaciol., 65, 1000–1010, https://doi.org/10.1017/jog.2019.77, 2019.

Iverson, N. R.: A theory of glacial quarrying for landscape evolution models, Geology, 40, 679–682, https://doi.org/10.1130/G33079.1, 2012.

Jansen, J., Knudsen, M., Andersen, J., Heyman, J., and Egholm, D.: Erosion rates in Fennoscandia during the past million years, Quaternary Science Reviews, 207, 37–48, https://doi.org/10.1016/j.quascirev.2019.01.010, 2019.

320 Jouzel, J., Masson-Delmotte, V., Cattani, O., Dreyfus, G., Falourd, S., Hoffmann, G., Minster, B., Nouet, J., Barnola, J. M., Chappellaz, J., Fischer, H., Gallet, J. C., Johnsen, S., Leuenberger, M., Loulergue, L., Luethi, D., Oerter, H., Parrenin, F., Raisbeck, G., Raynaud, D., Schilt, A., Schwander, J., Selmo, E., Souchez, R., Spahni, R., Stauffer, B., Steffensen, J. P., Stenni, B., Stocker, T. F., Tison, J. L., Werner, M., and Wolff, E. W.: Orbital and Millennial Antarctic Climate Variability over the Past 800,000 Years, Science, 317, 793–796, https://doi.org/10.1126/science.1141038, data archived at the World Data Center for Paleoclimatology, Boulder, Colorado, USA., 2007.

325 Kelly, M. A., Buoncristiani, J.-F., and Schlüchter, C.: A reconstruction of the last glacial maximum (LGM) ice surface geometry in the western Swiss Alps and contiguous Alpine regions in Italy and France, Eclogae geol. Helv, pp. 57–75, https://doi.org/10.1007/s00015-004-1109-6, 2004.

Kleman, J.: Preservation of landforms under ice sheets and ice caps, Geomorphology, 9, 19–32, https://doi.org/10.1016/0169-555x(94)90028-0, 1994.

330 Kleman, J., Stroeven, A. P., and Lundqvist, J.: Patterns of Quaternary ice sheet erosion and deposition in Fennoscandia and a theoretical framework for explanation, Geomorphology, 97, 73–90, https://doi.org/10.1016/j.geomorph.2007.02.049, 2008.

Kleman, J., Jansson, K., De Angelis, H., Stroeven, A., Hättestrand, C., Alm, G., and Glasser, N.: North American ice sheet build-up during the last glacial cycle, 115–21 kyr, Quaternary Sci. Rev., 29, 2036–2051, https://doi.org/10.1016/j.quascirev.2010.04.021, 2010.

Koppes, M., Hallet, B., Rignot, E., Mouginot, J., Wellner, J. S., and Boldt, K.: Observed latitudinal variations in erosion as a function of
335 glacier dynamics, Nature, 526, 100–103, https://doi.org/10.1038/nature15385, 2015.

Koppes, M. N. and Montgomery, D. R.: The relative efficacy of fluvial and glacial erosion over modern to orogenic timescales, Nature Geoscience, 2, 644–647, https://doi.org/10.1038/ngeo616, 2009.

Lane, S. N., Bakker, M., Gabbud, C., Micheletti, N., and Saugy, J.: Sediment export, transient landscape response and catchment-scale connectivity following rapid climate warming and alpine glacier recession, Geomorphology, 277, 210 – 227,
340 https://doi.org/10.1016/j.geomorph.2016.02.015, 2017.

Lisiecki, L. E. and Raymo, M. E.: A Pliocene-Pleistocene stack of 57 globally distributed benthic δ^{18}O records, Paleoceanography, 20, PA1003, https://doi.org/10.1029/2004pa001071, 2005.

MacGregor, K., Anderson, R., Anderson, S., and Waddington, E.: Numerical simulations of glacial-valley longitudinal profile evolution, Geology, 28, 1031–1034, https://doi.org/10.1130/0091-7613(2000)28<1031:NSOGLP>2.0.CO;2, 2000.

345 Margold, M., Jansson, K. N., Kleman, J., and Stroeven, A. P.: Glacial meltwater landforms of central British Columbia, J. Maps, 7, 486–506, https://doi.org/10.4113/jom.2011.1205, 2011.

Mariotti, A., Blard, P.-H., Charreau, J., Toucanne, S., Jorry, S., Molliex, S., Bourlès, D., Aumaitre, G., and Keddadouche, K.: Nonlinear forcing of climate on mountain denudation during glaciations, Nature Geoscience, pp. 1–7, https://doi.org/10.1038/s41561-020-00672-2, 2021.

350 Micheletti, N. and Lane, S. N.: Water yield and sediment export in small, partially glaciated Alpine watersheds in a warming climate, Water Resources Res., 52, 4924–4943, https://doi.org/10.1002/2016WR018774, 2016.

Moon, T., Joughin, I., Smith, B., and Howat, I.: 21st-Century Evolution of Greenland Outlet Glacier Velocities, Science, 336, 576–578, https://doi.org/10.1126/science.1219985, 2012.

Mouginot, J., Rignot, E., and Scheuchl, B.: Sustained increase in ice discharge from the Amundsen Sea Embayment, West Antarctica, from
355 1973 to 2013, Geophys. Res. Lett., 41, 1576–1584, https://doi.org/https://doi.org/10.1002/2013GL059069, 2014.

Overeem, I., Hudson, B. D., Syvitski, J. P. M., Mikkelsen, A. B., Hasholt, B., van den Broeke, M. R., Noël, B. P. Y., and Morlighem, M.: Substantial export of suspended sediment to the global oceans from glacial erosion in Greenland, Nature Geoscience, 10, 859–863, https://doi.org/10.1038/NGEO3046, 2017.

Penck, A.: Glacial Features in the Surface of the Alps, J. Geol., 13, 1–19, https://doi.org/10.1086/621202, 1905.

360 Ramsay, A. C.: On the Glacial Origin of certain Lakes in Switzerland, the Black Forest, Great Britain, Sweden, North America, and elsewhere, Q. J. Geol. Soc., 18, 185–205, https://doi.org/10.1144/gsl.jgs.1862.018.01-02.31, 1862.

Seguinot, J.: Glacial quarrying and development of overdeepenings in glacial valleys: modelling experiments and case studies at Erdalen, Western Norway, https://doi.org/10.31237/osf.io/8fzd6, 2008.

Seguinot, J.: Numerical modelling of the Cordilleran ice sheet, Ph.D. thesis, Stockholm University, http://urn.kb.se/resolve?urn=urn:nbn:se:
365 su:diva-106815, 2014.

Seguinot, J.: Alpine ice sheet glacial cycle simulations aggregated variables [data set], Zenodo, https://doi.org/10.5281/zenodo.3604174, 2020a.

Seguinot, J.: Alpine ice sheet glacial cycle simulations continuous variables [data set], Zenodo, https://doi.org/10.5281/zenodo.3604142, 2020b.

370 Seguinot, J.: Alpine ice sheet erosion potential aggregated variables [data set], Zenodo, https://doi.org/10.5281/zenodo.4495419, 2021.

Seguinot, J., Rogozhina, I., Stroeven, A. P., Margold, M., and Kleman, J.: Numerical simulations of the Cordilleran ice sheet through the last glacial cycle, The Cryosphere, 10, 639–664, https://doi.org/10.5194/tc-10-639-2016, 2016.

Seguinot, J., Ivy-Ochs, S., Jouvet, G., Huss, M., Funk, M., and Preusser, F.: Modelling last glacial cycle ice dynamics in the Alps, The Cryosphere, 12, 3265–3285, https://doi.org/10.5194/tc-12-3265-2018, 2018.

375 Steinemann, O., Ivy-Ochs, S., Grazioli, S., Luetscher, M., Fischer, U. H., Vockenhuber, C., and Synal, H.-A.: Quantifying glacial erosion on a limestone bed and the relevance for landscape development in the Alps, Earth Surf. Processes and Landforms, 45, 1401–1417, https://doi.org/10.1002/esp.4812, 2020.

Steinemann, O., Ivy-Ochs, S., Hippe, K., Christl, M., Haghipour, N., and Synal, H.-A.: Glacial erosion by the Trift glacier (Switzerland): Deciphering the development of riegels, rock basins and gorges, Geomorphology, 375, 107 533,
380 https://doi.org/10.1016/j.geomorph.2020.107533, 2021.

the PISM authors: PISM, a Parallel Ice Sheet Model, http://www.pism-docs.org, 2017.

Thomson, S., Brandon, M., Tomkin, J., Reiners, P., Vásquez, C., and Wilson, N.: Glaciation as a destructive and constructive control on mountain building, Nature, 467, 313–317, https://doi.org/10.1038/nature09365, 2010.

Tulaczyk, S., Kamb, W. B., and Engelhardt, H. F.: Basal mechanics of Ice Stream B, west Antarctica: 1. Till mechanics, J. Geophys. Res.,
385 105, 463, https://doi.org/10.1029/1999jb900329, 2000.

Ugelvig, S., Egholm, D., Anderson, R., and Iverson, N.: Glacial erosion driven by variations in meltwater drainage, J. Geophys. Res. Earth Surf., 123, https://doi.org/10.1029/2018JF004680, 2018.

Werder, M. A., Hewitt, I. J., Schoof, C. G., and Flowers, G. E.: Modeling channelized and distributed subglacial drainage in two dimensions, J. Geophys. Res. Earth Surf., 118, 2140–2158, https://doi.org/10.1002/jgrf.20146, 2013.

390 Willenbring, J. and Von Blanckenburg, F.: Long-term stability of global erosion rates and weathering during late-Cenozoic cooling, Nature, 465, 211–214, https://doi.org/10.1038/nature09044, 2010.

Wirsig, C., Zasadni, J., Christl, M., Akçar, N., and Ivy-Ochs, S.: Dating the onset of LGM ice surface lowering in the High Alps, Quaternary Sci. Rev., 143, 37–50, https://doi.org/10.1016/j.quascirev.2016.05.001, 2016.

Zekollari, H. and Huybrechts, P.: On the climate–geometry imbalance, response time and volume–area scaling of an alpine
395 glacier: insights from a 3-D flow model applied to Vadret da Morteratsch, Switzerland, Annals of Glaciology, 56, 51–62, https://doi.org/10.3189/2015aog70a921, 2015.